SPECTROSCOPIC AND ELECTROCHEMICAL PROPERTIES OF 1,3-DIKETONATOBORON DERIVATIVES

YUAN L. CHOW, CARL I. JOHANSSON, YU-HUANG ZHANG, RENE GAUTRON, LI YANG, ANDRE RASSAT AND SHI-ZHU YANG

Department of Chemistry, Simon Fraser University, Burnaby, BC, V5A 1S6, Canada.

A series of tetracoordinated boron complexes derived from various 1,3-diketones and bidentate ligands (oxalato, malonato, catecholato and difluoro) were prepared. Their absorption, fluorescence and phosphorescence spectra, at ambient temperature and 77 K, and cyclic voltammmetry in acetonitrile were studied. The boron complexes exhibited high molar absorptivity and fluorescence intensities as compared with the parent diketones; the phenomena are in agreement with the lowest singlet excited state possessing the $\pi, \pi,^*$ configuration with a rigid chelate structure. The redox potential differences correlate linearly with the lowest singlet (E_S) as well as the triplet (E_T) excited state energy with slopes lower than unity. These linear correlations re-state that the electron exchange and Coulombic integral also vary proportionally to the potential differences. From these correlations, it is possible to determine E_S and E_T of those boron complexes that do not give fluorescence and phosphorescence.

INTRODUCTION

Tetracoordinated borates derived from a molecule of 1,3-diketones and contributing bidentate anionic portions derive their stability from the extensive resonance of alternating dative and covalent bonds of diketones.[1] The structures **1–4** are the borates prepared and studied in this work; the diketones are derived mainly from acetylactone (AAH), benzoylacetone (BAH), dibenzoylmethane (DBMH) and its substituted derivative (MBDH). The bidentate group of the 1,3,2-dioxaborole moiety is derived from oxalic acid, malonic acid and catechol. The corresponding difluoro derivatives possess relatively unreactive B—F bonds and have been investigated infrequently since 1905.[2]
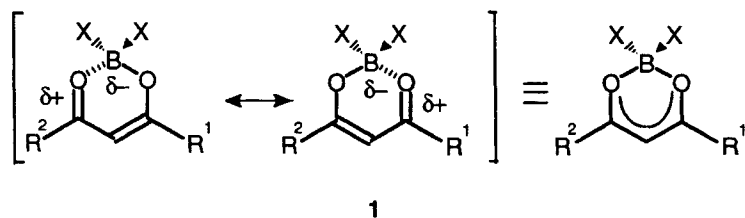
We have recently discovered that BF_2 complexes (**2**, **3** and **4**) exhibit synthetically useful 2 + 2 photocycloaddition and photoinduced electron transfer (i.e. radical ion) reactions and also, mechanistically, exhibiting fluorescent excimer and exciplex phenomena.[3] As interest in the photochemistry and photophysics of boron complexes is mounting, it became pertinent to clarify their spectroscopic and redox properties as a basis for understanding their reactions and phenomena. This paper deals with the spectroscopic (absorption and emission) and electrochemical (redox potentials) properties of the boron complexes **1–4**.
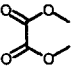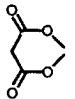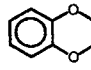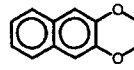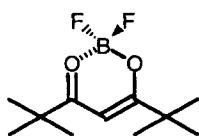
RESULTS

Emission studies

The borates **1** derived from fluoride, oxalate and catechol have been prepared previously[3,4] and their absorption properties been reported under a variety of conditions.[2–4] Using similar preparative conditions, borates **1** derived from malonic acid and naphthalene-2,3-diol were also prepared, the latter primarily for another study.[5]
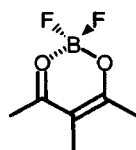
The principal absorption band and intensity of these boron complexes are summarized in Table 1, in which the corresponding 1,3-diketone *cis*-enol tautomer data are also given. For the latter, whenever possible, their observed molar absorptivity was corrected for the percentage of the *cis* tautomer in solution;[5] the corrected values are given in parentheses. All of the boron complexes showed significant enhancement in ε_{max} along with bathochomic shifts in the range 10–40 nm relative to their corresponding parent diketones. The bathochromic shifts were larger with increasing conjugation, i.e. AA < BA < DBM < MBD in each series. The bidentate counter ligand did not affect the absorption maxima significantly. The large molar absorptivities in comparison with those of their parent diketones and also, in some cases, spectral vibrational structure
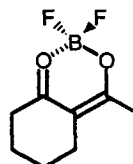
1

R^1, R^2 \ X,X	F,F				
CH$_3$, CH$_3$	AABF$_2$	AABO	AABM	AABC	AABN
C$_6$H$_5$, CH$_3$	BABF$_2$	BABO	BABM	BABC	BABN
C$_6$H$_5$, C$_6$H$_5$	DBMBF$_2$	DBMBO	DBMBM	DBMBC	DBMBN
p-CH$_3$O-C$_6$H$_5$, p-t-Butyl-C$_6$H$_5$	MBDBF$_2$	MBDBO	MBDBM	MBDBC	MBDBN

2   **3**   **4**

support the assignment of the principal absorption as the $\pi-\pi^*$ transition of the diketonate ligand. This is further supported by the observation that substitution of the olefinic hydrogen with an alkyl group showed a large bathochromic shift (as in **3** and **4**), but that of the methyl hydrogen (as in **2**) caused no change.

One noteworthy phenomenon was the deeper color of catecholatoboron derivatives in comparison with the other complexes. For example, AABF$_2$-MBDBF$_2$ (and the oxalato and malonato series) ranged from colourless to pale yellow solids, whereas the color of AABC, BABC, DBMBC, and MBDBC grew progressively deeper, namely ranging from yellow, orange, reddish orange to dark red. An examination of the UV-visible absorption spectra of the catecholatoboron derivatives

reveals weak and broad band beyond the principal absorption band, which is assigned as a charge-transfer band (CT). The spectra of DBMBF$_2$ and DBMBC are shown in Figure 1, where the latter clearly reveals the CT band. Such CT absorption bands were studied in separate work[5] dealing with similar borates derived from naphthalene-2,3-diol as the bidentate ligand (the BN series) and will not be repeated here.

There are scattered reports on the fluorescence spectra of BF$_2$ and oxalatoboron complexes.[6] From the necessity for mechanistic studies related to their photochemistry, the fluorescence properties of DBMBF$_2$ and AABF$_2$ were also studied in depth recently.[3b,7] Fluorescence (emission and excitation) and phosphorescence spectra of boron complexes were studied mainly in acetonitrile

Table 1. Principal absorption bands of 1,3-diketonatoboron complexes and the corresponding parent 1,3-diketones in UV−visible spectra

Compound	λ_{max} (nm)	Log ε_{max} (corr.)[a]	Compound	λ_{max} (nm)	Log ε_{max} (corr.)[a]
DBMBF$_2$	363	4·61	BABO	334[d]	4·25
	364[b]	4·55	AABO	288[d]	4·09
	359[c]	4·53	DBMBM	370	4·57
MBDBF$_2$	400	4·82	MBDBM	410	4·82
	401[b]	4·78	BABM	332	4·43
	392[c]	4·72	AABM	288	4·15
BABF$_2$	328	4·43	DBMBC	368	4·62
AABF$_2$	283	4·13	MBDBC	401	4·72
	285[d]	4·24	BABC	334	4·28
ACHBF$_2$	304[b]	4·15	AABC	287	4·13
D-t-BBF$_2$	284	4·09	DBMBN	363[e]	4·60
Me-AABF$_2$	3·02	4·20	MBDBN	406	4·66
DBMBO	371	4·60	BABN	331	4·35
MBDBO	414	4·80	AABN	282	4·19
DBMH	342	4·38 (4·44)	AAH	273	3·83 (4·11)
	338[c]	4·39 (4·40)		275[d]	3·93 (4·01)
MBDH	356	4·51[f]		273[c]	4·03 (4·04)
	350[c]	4·51[f]			
BAH	310	4·14 (4·21)	ACHH	284	3·91[f]
	305[c]	4·26 (4·27)			

[a] Data in parentheses are corrected for the percentage of cis-enol tautomer[5] by dividing the experimental ε_{max} by this percentage.
[b] Unless stated otherwise, spectra were recorded in acetonitrile.
[c] In dichloromethane.
[d] In cyclohexane.
[e] In 1,2-dichloroethane.
[f] Percentage in acetonitrile of cis-enol tautomer unknown.

and in methylcyclohexane glass at 77 K. As the catecholatoboron complexes showed complex fluorescence patterns that are excitation wavelength dependent, they were studied separately.[5] The normalization of the fluorescence emission and excitation spectra were used to determine the 0—0 band and, in turn, the spectroscopic singlet excited state energy (Figure 2). The spectroscopic triplet excited-state energy was calculated from the phosphorescence onset. These data are summarized in Table 2. The fluorescence quantum yield was determined by the optically dilute method using anthracene as a fluorescence standard.[7] The fluorescence lifetime was determined by time-correlated single photon counting using the PTI LS-1 (see Experimental).

For the BF$_2$, oxalatoboron and malonatoboron complex series, the fluorescence intensities (at room temperature) increased in the order AA < BA < DBM < MBD. The complexes with the AA ligand gave either no (for AABF$_2$ and AABO) or very weak (for AABM) fluorescence. Total emission in methylcyclohexane glass at 77 K was also acquired; for DBMBF$_2$, in spite of a low fluorescence quantum yield of $\Phi_F = 0·045$ in cyclohexane

at room temperature, it exhibited a strong and structured fluorescence $(\Phi_F = 0·9)^{[8]}$ in glassy solution at 77 K with a weak phosphorescence signal (Figure 3). MBDBF$_2$ showed a similar total emission spectrum to Figure 3. In contrast, BABF$_2$ showed both fluorescence and phosphorescence emissions with about equal intensity, but AABF$_2$ showed no luminescence. For their parent diketones, DBMH and MBDH showed weak fluorescence whereas AAH and BAH showed no detectable fluorescence at 77 K; all of them showed phosphorescence emission.

Electrochemical studies

Because redox potentials are important parameters to evaluate the extent of electron donor−acceptor interactions, these boron complexes were investigated by cyclic voltammetry (CV) in acetonitrile with respect to an SCE reference electrode (see Experimental). At a scan rate of 100 mV s^{-1} the oxidation CV curves were all irreversible. The reduction CV curves were mostly irreversible except for those marked with an asterisk, which were quasi-reversible, that is, the difference in
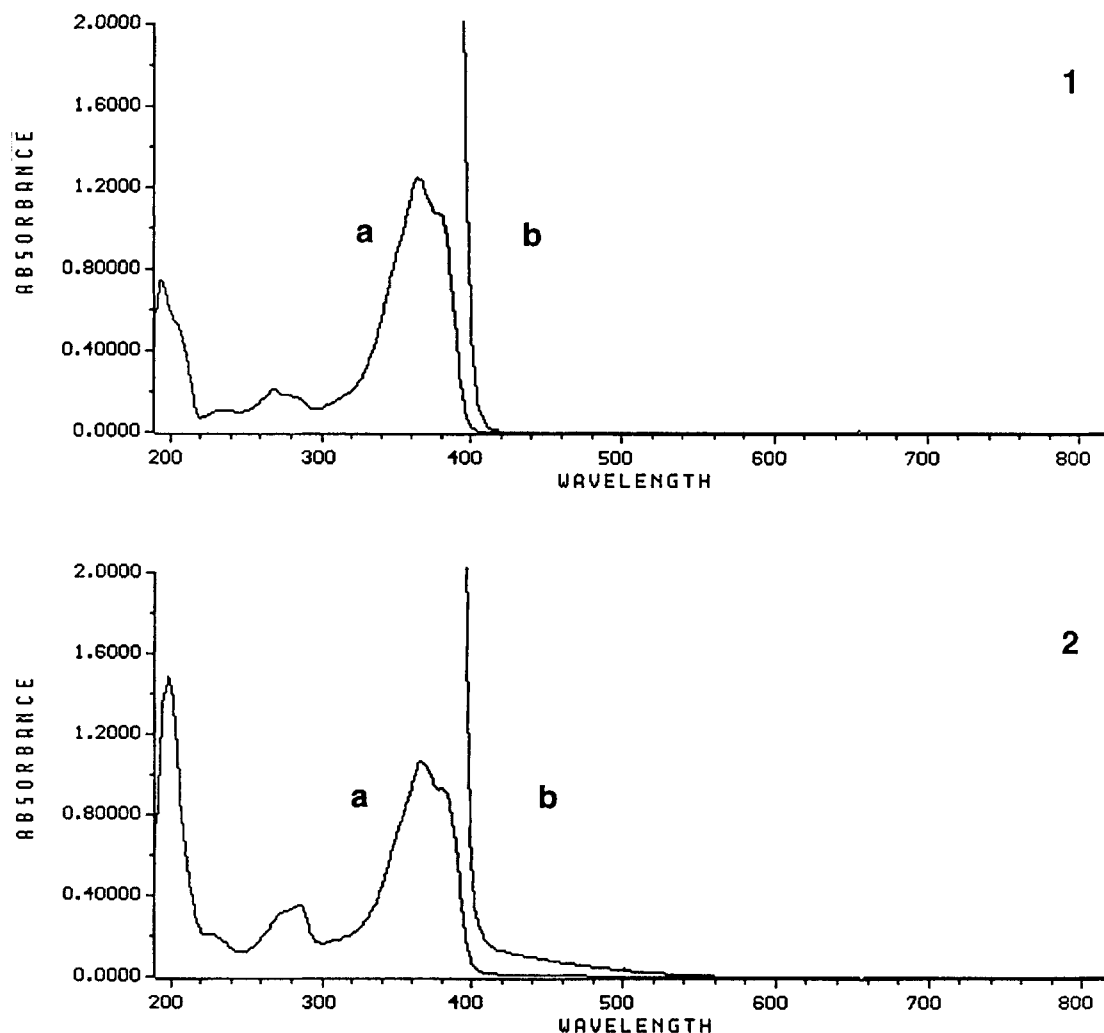
Figure 1. Absorption spectra in CH_3CN: (1) $DBMBF_2$ at (a) 2.9×10^{-5} M and (b) 2.9×10^{-4}; (2) DBMBC at (a) 2.5×10^{-5} M and (b) 2.5×10^{-4} M

Epa and Epc was scan rate dependent and greater than 60 mV.[9] The complexes with a 2,3-dihydroxynaphthalene ligand (the BN series) were also available from another study[5] and were also included in the redox study. It is known that for $AABF_2$ and $DBMBF_2$, in monogylme, the reduction involves the transfer of one electron so that $DBMBF_2$ forms a stable anion radical.[10]

With respect to their parent diketones, the boron complexes (BF_2, oxalato and malonato derivatives) were more difficult to oxidize at 0.6–0.8 V but more easily reduced at 0.3–0.5 V. In addition, the variation in reduction potentials systematically followed the extent of diketonate ligand conjugation within the same series (e.g. compare the E_{red} change for the BF_2 complex series). It was concluded that for these complexes the first reduction occurred in the diketonate ligand. AABO appeared to be an exception, showing two reduction peaks at −0.89 and −1.10 V vs SCE. The former appears to arise from the reduction of the oxalato ligand and the latter from the diketonate ligand (see below). A weak second wave at −0.95 V was also observed for BABO, but the other oxalatoboron complexes did not show a second reduction peak under the experimental conditions.

Both catecholatoboron and naphthalenediolatoboron complexes, as a group, exhibit a similar trend in
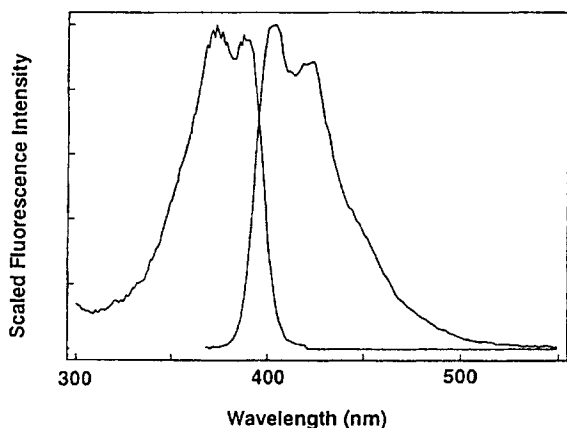
Figure 2. Normalized fluorescence emission and excitation spectra (corrected) of DBMBO $(4 \times 10^{-7}$ M$)$ in oxygen-free CH_3CN

reduction potentials as the BF_2, oxalato and malonato derivatives. However, catecholatoboron and naphthalenediolatoboron complexes show oxidation potentials that were less positive and did not significantly vary from one complex to another, irrespective of the diketonate ligand. For example, the naphthalenediolatoboron complexes gave similar oxidation potentials, within experimental error, that were similar to that of the methyl ether of naphthalene-2,3-diol (Table 3) but significantly lower than those of the diketonate ligands (e.g. the lowest diketonate ligand oxidation was ca. 1·97 V for the MBD ligand). Similar observations could be made for catecholatoboron complexes. It was clear that in these complexes the catecholate or naphthalenediolate ligand was the common entity participating in electron donation and more easily oxidized. To test this proposal, the oxidation range was extended beyond the first oxidation for DBMBN up to +2·8 V, which gave two other oxidation peaks at 1·39 and 2·45 V vs SCE. The latter clearly correlated with $E_{ox} = 2·45$ V observed for the DBM complexes with the BF_2, oxalatoboron and malonatoboron.

Table 2. Excited-state parameters from fluorescence (in acetonitrile) and phosphorescence (in methylcyclohexane at 77 K)

Complex	Singlet parameters			Triplet parameters		
	λ_F (nm)	E_S (eV)	Φ_Φ^α	τ (ns)	λ_p (nm)	E_T (eV)
AABF$_2$	—	4·18[a](4·12)	—	<0·01	—	3·21[b]
Me-MBF$_2$	—	3·73[b](3·70)	—	—	—	2·92[b]
D-t-BBF$_2$	—	4·13$_b$(4·10)	—	—	390	3·18
ACHBF$_2$	326	3·80	<0·01	<0·3	429	2·89
BABF$_2$	350	3·54	0·007	<0·3	444	2·79
DBMBF$_2$	383[c];389	3·24[c];3·19	0·045[c],0·092	0·23[c],0·28	461	2·69
MBDBF$_2$	416	2·98	0·43	2·01	508	2·44
AABO	—	3·88[b](4·04)	<10^{-4}	—	—	3·01[b]
BABO	358	3·46	<10^{-3}	—	454	2·73
DBMBO	399	3·11	0·41	1·35	—	2·52[b]
MBDBO	435	2·85	d	1·78	519	2·39
AABM	—	3·91[b](4·04)	<10^{-4}	—	381	3·25
BABM	357	3·47	<10^{-3}	—	459	2·70
DBMBM	396	3·13	0·32	0·86	473	2·62
MBDBM	435	2·85	d	2·14	539	2·30
AABC	—	4·14[b](4·13)	—	—	—	3·18[b]
BABC	—	3·55[b](3 54)	—	—	—	2·81[b]
DBMBC	—	3·30[b](3·18)	<0·01	—		2·63[b]
MBDBC	—	2·98[b](2·92)	<0·01	—		2·43[b]
DBMBAc$_2$	~390[e]	~3·18[e]	0·8[e]	1·5[e]	476[e]	2·60[e]
AAH	317	3·90[b](4·25)			383	3·24
BAH	372	3·33[b](3·54)			470	2·64
DBMH	409	3·03[b],3·23			480	2·58
MBDH	392	3·16	<0·01		482	2·57

[a] Where no data are given, unless stated otherwise, the compounds give no detectable luminescence under conventional conditions: the data in parentheses are calculated from the absorption onset.
[b] Calculated from equations obtained from regression analysis of Figure 5; $E_S = 0·54 + 0·84(E_{ox} - E_{red})$; $E_T = 0·89 + 0·53(E_{ox} - E_{red})$.
[c] Measured incyclohexane.
[d] Fluorescenceyields notmeasured.
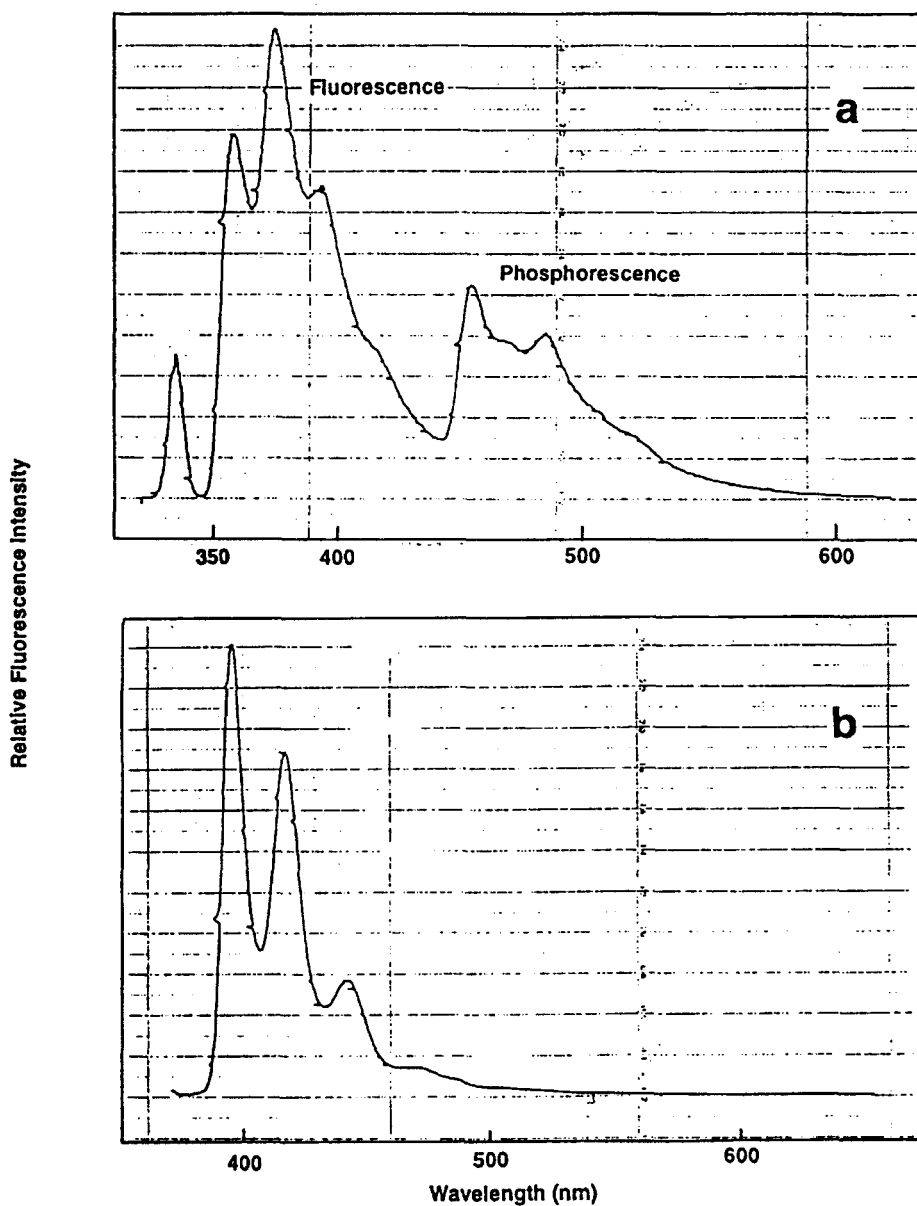[e] Dibenzoylmethanatoboron diacetate; the data are cited from Ref. 6a.

Figure 3. Total emission spectra (uncorrected) of (a) $BABF_2$ $(2\cdot8 \times 10^{-4}$ M) and (b) $DBMBF_2$ $(9\cdot6 \times 10^{-6}$ M) in methylcyclohexane glass at 77 K. The peak at 355 nm for (a) is the Rayleigh band

The observed irreversible redox potentials for boron complexes in this study were believed to be due to a rapid irreversible chemical reaction[10] that depleted the concentration of the ion radical species at the electrode surface before reverse electron transfer could occur, i.e. an electron transfer–chemical reaction mechanism (EC).[9] However, no film or deposit on the platinum working electrode surface was detected. Although irreversible CV renders the redox potentials in Table 3 less reliable, every series show systematic variations along structural changes. These data can therefore be used in correlative studies (see below). In the reduction of boron complexes, the anion radicals could be more stable by virtue of either conjugation or the absence of

Table 3. Redox potentials of some boron complexes in acetonitrile[a]

Compound	E_{ox} (V)	$-E_{red}$ (V)	Compound	E_{ox} (V)	$-E_{red}$ (V)
DBMBF$_2$	2·45	0·91[b]	DBMBN	1·18,1·39,2·45	0·81[b]
BABF$_2$	2·53	1·13	BABN	1·20	1·01
MBDBF$_2$	1·96	1·01[b]	AABN	1·20	1·36
AABF$_2$	2·88	1·48	MBDBN	1·11	0·91
Me-AABF$_2$	2·34	1·48	DBMBM	2·43	0·70
ACHBF$_2$	2·30	1·50	BABM	2·50	0·88
D-t-BBF$_2$	2·80	1·50	AABM	2·81	1·23
DBMBO	2·43	0·64	MBDBM	1·98	0·83
BABO	2·60	0·80(0·95)[c]	DBMH	1·60[d]	1·38[e]
AABO	2·90	0·89,1·10	BAH	1·80[d]	1·54[e]
MBDBO	1·97	0·78	AAH	2·25	1·78
DBMBC	1·05	0·85[b]			
BABC	1·07	1·06	2,3-DMN	1·39	
AABC	1·10	1·42	o-DMB	1·45	
MBDBC	1·10	0·94			

[a] Obtained at ambient temperature under nitrogen with 0·1 M TEAP vs the SCE reference electrode; scan rate 100 mV s^{-1}. Errors ±0·05 V.
[b] Quasi-reversible cyclic voltammograms.
[c] Possible second wave.
[d] Calculated from equation (1) in which unknowns are estimated to be 0·22 V.
[e] Ref. 10b.

α-hydrogens, that is, the reverse scan peak is observable. The fact that D-t-BBF$_2$ (2) showed a quasi-reversible reduction undoubtedly reflected the absence of α-hydrogens coupled with inherent steric hindrance to protect from an attacking species on the anion radical.

DISCUSSION

Both the emission and absorption spectra of boron complexes show the expected bathochromic progression as the conjugation is extended as shown in the structure. Various observations reported above indicate that these boron complexes possess a $\pi-\pi^*$ transition as the lowest excited state; the observations are, for example, (i) fluorescence and absorption bathochromic shift with increasing solvent polarity, (ii) large ε_{max} and (iii) large single triplet energy gaps (ΔE_{ST}) as shown in Tables 2 and 3. The π, π^* configuration for the lowest singlet excited state can be rationalized on the basis of chelation effects.

Chelation has been used extensively in the analysis of metal ion concentrations by either absorption or emission spectroscopy.[11] For fluorimetry, an ideal case is that while a chelating agent is non- or weakly fluorescent, its metal complex is strongly fluorescent. The chelative complex formation in borates utilizes the non-bonding electrons on the carbonyl oxygen in coordination with the boron vacant p-orbital. and results in a resonance-stabilized ring where the n-electrons are lowered considerably and the highest energy π-orbital becomes the HOMO. Supporting evidence for the chelate formation in BF$_2$ complexes has been discussed

on the basis of x-ray crystallography[12] and IR[10,13] and NMR spectroscopic data in previous papers.[3] It is certain that the AAH and BAH series follow this pattern, where the parent compounds have the n,π^* configuration[14] as the lowest singlet excited state, but the corresponding boron complexes have the π, π^* configuration. However, evidence suggests that the DBMH[14b] and MBDH diketones have the π, π^* configuration for the lowest singlet excited state, which is known to undergo a large amplitude twisting motion[15] that degrades the excitation energy into thermoenergy, whence the lack of fluorescence at room temperature. This twisting motion can be inhibited in rigid methyl-cyclohexane glass, which allows fluorescence from DBMH and MBDH to be easily detected. The rigidty of the chelated structure and increased conjugation prevent this twisting motion and thus the fluorescence can be observed.

The variation in luminescence yields (or relative intensities) for the BF$_2$ series in a glassy matrix at 77 K (Figure 3) are probably related to rates of the non-radiative processes. The lack of emission in AABF$_2$ has been suggested to be due to a fast internal conversion of the singlet excited state even under frozen conditions.[7] As seen in Figure 3, the increased relative phosphorescence intensity of BABF$_2$, as compared with that of DBMBF$_2$, is noteworthy and must arise from an increased intersystem crossing rate for BABF$_2$. This may be brought about by the lowering of the singlet excited state energy close to the second triplet state (T$_2$ or n, π^*) wherein the probability of the intersystem crossing is enhanced by virtue of a small ΔE_{ST} following the S$_1 \rightarrow$T$_2 \rightarrow$T$_1$ path. In DBMBF$_2$, increased

conjugation brings the lowest singlet energy level below the T_2 level; this naturally eliminates the above advantage. In general, a slow intersystem crossing rate can result in a high fluorescence intensity by a competing fluorescence rate.

The coordination of the non-bonded electrons on the diketonate oxygens to form a tetracoordinated borate results in a diketonate ligand with a local C_{2v} symmetry. This is demonstrated by identical C—O, C—C and B—O bond lengths[12] even for the unsymmetrical complexes containing the BA ligand.[12b] On the basis of the C_{2v} symmetry, the diketonate ring has been studied by the Huckel LCAO–MO treatment and the π-electron coefficients, energy levels and electron densities have been calculated (Figure 4).[16] This calculation shows an noteworthy feature that the methine position coefficient is zero in the LUMO but large in the HOMO. Therefore, substitution at the methine position does not electronically affect the LUMO energy but should affect the HOMO energy. This is exactly what is observed in the reduction potentials of Me-AABF$_2$, D-t-BBF$_2$, ACHBF$_2$ and AABF$_2$ (Table 3): methyl substitution at the methine position results in a lowering of the oxidation potential but the corresponding reduction potential remains the same within experimental error.

The primary objective of this investigation is to develop an interrelationship between the spectroscopic and electrochemical characteristics of these boron complexes. The energy levels of the lowest excited states (singlet and triplet) have been theoretically interrelated to the HOMO and LUMO energy levels,[17] that are, in turn, correlated to the redox potentials. The singlet and triplet state energies, E_S and E_T, can be expressed in terms of the difference in redox potentials as follows:[18]

$$E_S = E_{ox} - E_{red} + \Delta\Delta G_{solv} - J + 2K \quad (1)$$

$$E_T = E_{ox} - E_{red} + \Delta\Delta G_{solv} - J \quad (2)$$

$$E_S - E_T = 2K = \Delta E_{ST} \quad (3)$$

where K and J are the exchange integral and the Coulombic integral, respectively, and $\Delta\Delta G_{solv}$ is the difference in solvation free energies of the radical anion and cation. These equations have been used to
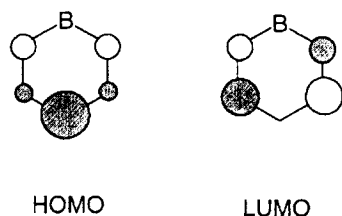
determine K [equation (3)] and to estimate J from the relevant data of structurally related compounds with some success.[18a] The success is due, in part, to a relatively constant $\Delta\Delta G_{solv}$ term, which does not vary beyond 0·2 eV.[19] Figure 5 shows the plots according to equations (1) and (2), using the experimental data in Tables 2 and 3.

The triplet energies, E_T, show a good linear relationship with the redox potential difference with a slope of 0·53 and a y-intercept of 0·89. The singlet energies, E_S, show a more scattered linear trend with a slope of 0·84 and a y-intercept of 0·54. The slope of less than unity suggests that the Coulombic integral decreases systematically concurrent with decreasing potential differences. This should be expected since an increase in conjugation causes a decrease in potential difference and also in the J and K integrals in a systematic manner; for the present purpose, the J and K terms are set as linear functions of the redox potentials difference:[18a]

$$J = a + b(E_{ox} - E_{red}) \quad (4a)$$

$$2K = c + d(E_{ox} - E_{red}) \quad (4b)$$

Equations (4a) and (4b) are incorporated into equations (1) and (2) to give equations (5) and (6), respectively:

$$E_s = (1 - b + d)(E_{ox} - E_{red}) + \text{constant} \quad (5)$$

$$E_T = (1 - b)(E_{ox} - E_{red}) + \text{constant} \quad (6)$$

As shown in Figure 5, the energy gap ΔE_{ST} narrows, that is, the K integral becomes smaller as required by equation (3) as the redox potential difference becomes smaller. The K integral is a relative measure of how an electron in the HOMO and an electron in the LUMO come in contact with each other.[20] As increasing conjugation increases the redox potential difference that, in

Figure 4. Hückel LCAO–MO description of the acetylacetone 1,3-diketonatoboron moiety. The size of the orbital indicates the relative magnitude of the orbital coefficient
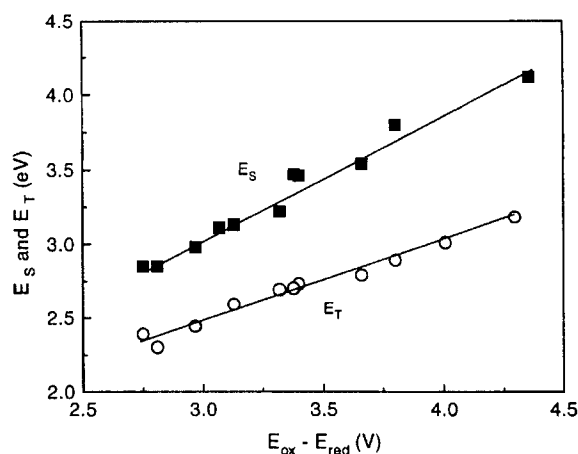

Figure 5. Correlation of the lowest singlet and triplet excited-state energy levels vs redox potential differences. The regression analysis gives $E_S = 0·54 + 0·84(E_{ox} - E_{red})$ and $E_T = 0·89 + 0·53(E_{ox} - E_{red})$

turn, reduces the extent of the type of contact, the smaller value of E_{ox}-E_{red} reduces the K integral.

AABO possess two reduction potentials at -0.89 and -1.10 V. The latter is shown to be correlated better with the singlet and triplet energies in Figure 5, that is, the -1.10 V value gives a better agreement for E_S and E_T correlations according to equations (1) and (2). On the basis of these correlations, the AABO reduction potential at -1.10 V is assigned to electron addition to the AA diketonatoboron moiety. It follows that the potential at -0.89 V may arise from the reduction of the oxalatoboron moiety. The weak wave of BABO ≈ -0.95 V should therefore be the reduction potential of the BO moiety. We are not able to rationalize why a second wave was not observed for other BO complexes.

The correlation plots in Figure 5 can be used to estimate the singlet and triplet energy levels of boron complexes when their emission is lacking. For those borates that show no fluorescence and/or phosphorescence, their singlet and triplet energies were read from Figure 5 and are shown in Table 2; E_S obtained in this way compared well with the data estimated from the onset of the absorption spectra.

EXPERIMENTAL

Materials. Boron complexes were prepared and recrystallized according to published procedures.[3,4] Solvents were of spectrograde quality and were used without further purification: acetonitrile, carbon tetrachloride (BDH), chloroform (Fisher), dichloromethane, cyclohexane (Mallicrodkt) and methylcyclohexane (BDH).

Instrumentation. Fluorescence emission and excitation spectra were recorded at ambient temperature (23 ± 1 °C) on a PTI LS-100 fluorimeter (corrected). Solutions (1×10^{-6}–3×10^{-6} M for DBMBX and MBDBX compounds, 1×10^{-4}–5×10^{-4} M for BABX and AABX compounds) were purged with argon for several minutes in a 1 cm path-length cell sealed with a rubber septum before measurement. Phosphorescence spectra were recorded on a Perkin-Elmer MPF–44B fluorimeter (uncorrected) with a Hitachi phosphorescence unit; low-temperature fluorescence (77 K) was performed with the same apparatus without the chopper. Lifetime data were obtained on a PTI LS-1, the procedure of which has been described previously.[21]

Cyclic voltammetry. Cyclic voltammetry was performed using a three-electrode arrangement with an SCE reference electrode (Fisher), a stationary Pt working electrode (surface area 0.018 cm^2) and a Pt counter electrode. The electronics included a Princeton Applied Research (PAR) Model 173 programmer, a

PAR Model 178 electrometer and a PAR Model 173 potentiostat/galvanostat equipped with a PAR Model 179 digital coulometer that provided feedback compensation for the ohmic drop between the working and reference electrodes. Cyclic voltammograms were recorded on a Allen recorder. The electrochemical cell was based on the design of Kissinger and Heineman,[22] but adapted with a Luggin–Haber tube to reduce the ohmic drop. Acetonitrile was refluxed and distilled over CaH$_2$ under argon. The concentration of the electroactive species was 2–3 mM. The electrolyte was tetraethylammonium perchlorate (GFS Chemicals, support electrolyte grade; 0.1 M). The reported redox potentials were calibrated with respect to the ferrocene–ferrocenium couple. The experimental range of the apparatus was determined, in the absence of an electroactive species, to be -2 to $+3$ v (100 mVs^{-1}).

REFERENCES

1. W. Gerrard, M. F. Lappert and R. Shafferman, *Chem. Ind. (London)* 722 (1958).
2. R. C. Mehrota, R. Bohra and D. P. Gaur, *Metal β-Diketonates and Allied Derviatives.* Academic Press, New York (1978).
3. (a) Y. L. Chow and X. Cheng, *Can. J. Chem.* **69**, 1575 (1991); (b) Y. L. Chow, X. Cheng and C. I. Johansson, *J. Photochem. Photobiol.* A **57**, 247 (1991); (c) Y. L. Chow, S.P. Wu and X. Ouyang, *J. Org. Chem.* **59**, 421 (1993).
4. H. Hartmann *J. Prakt. Chem.* **328**, 755 (1986).
5. C. I. Johansson, PhD, Thesis, Simon Fraser University (1994).
6. (a) H.-D. Ilige, E. Bircker, D. Fassler, M. V. Kozmenko, M. G. Kuz'min and H. Hartmann, *J. Photochem.* **32**, 177 (1986); (b) H.-D. Ilige, M. V. Kozmenko, M. G. Kuz'min and H. Hartmann, *J. Photochem.* **36**, 27 (1987); (c) H.-D. Ilige, D. Fassler and H. Hartmannm, *Z. Chem.* **24**, 218 (1984); (d) H.-D. Ilige, D. Fassler and H. Hartmann, *Z. Chem.* **24**, 292 (1984); (e) V. E. Karasev and O. A. Korotkikh, *Russ. J. Inorg. Chem.* **30**, 1290 (1985); (f) V. E. Karasev and O. A. Korotkikh, *Russ. J. Inorg. Chem.* **31**, 493 (1986); (g) A. M. Brouwer N. A. Bakker, P. G. Wiering and J. W. Verhoeven, *J. Chem. Soc., Chem. Commun.* 1094 (1991).
7. Y. L. Chow and C. I. Johansson, *Chem Phys. Lett.* **231**, 541 (1994).
8. K. Gustav and M. Storch, Monatsh. Chem. **121**, 447 (1990).
9. D. T. Sawyer and J. L. Roberts, Jr, *Experimental Electrochemistry for Chemists.* Wiley, New York (1986).

10. (a) L. H. Toporcer, R. E. Dessy and S. I. E. Green. *Inorg. Chem.* **4**, 1649 (1965); (b) R. C. Buchta and D. H. Evans. *Anal. Chem.* **40**, 2181 (1968).

11. D. A. Skoog, D. A. *Principles of Instrumental Analysis.* Saunders, Philadelphia (1985).

12. (a) R. Boese, R., Köster and M. Yalpani, M. *Chem. Ber.* **118**. 670 (1985); (b) A. W. Hanson and E. W. Macaulay, *Acta. Crystallogr., Sect. B* **28**, 1961 (1972); (c) F. A. Cotton and W. H. Ilsley, *Inorg. Chem.* **21**, 300 (1982); (d) S. J. Rettig and J. Trotter, *Can. J. Chem.* **54**, 1168 (1976); (e) S. J. Rettig and J. Trotter, *Can. J. Chem.* **60**, 2957 (1982).

13. N. M. B. Brown and P. Bladon. *J. Chem. Soc.* A 526 (1969).

14. (a) H. Nakanishi, H., Morita and S. Nagakura. *Bull. Chem. Soc. Jpn*, **50**, 2255 (1977); (b) P. Gacoin, *J. Chem. Phys.* **57**, 1418 (1972).

15. (a) P. Markov, *Chem. Soc. Rev.* **69**, 69 (1984); (b) D. Veierov, T. Beercovici, Y. Mazur and E. Fischer, *J. Org. Chem.* **43**, 2006 (1978).

16. R. L. Belford, A. E. Martell and M. Calvin, *J. Inorg Nucl. Chem.* **2**, 11 (1956).

17. A. Streitwieser, Jr, *Molecular Orbital Theory for Organic Chemists.* Wiley, New York (1961).

18. (a) R. O. Loutfy and R. O., Loutfy, *Can. J. Chem.* **54**, 1454 (1976); (b) T. Kubota, H. Miyazaki, M. Yamakawa, K. Ezumi, and Y. Yamamoto, *Bull. Chem. Soc. Jpn.* **52**, 1588 (1979).

19. J. R. Wiley, E. C. M. Chen, E. S. D. Chen, P. Richardson, W. R. Reed and W. E. Wentworth, *J. Electroanal. Chem.* **307**, 169 (1991).

20. J. Michl and V. Bonacic-Koutecky, *Electronic Aspects of Organic Photochemistry.* Wiley–Interscience, New York (1990).

21. Y. L. Chow and C. I. Johansson, J. Photochem. Photobiol. A **74**, 171 (1993).

22. P. T. Kissinger and W. R. Heineman, *J. Chem. Educ.* **60**, 702 (1983).